Distorted antibody repertoire developed in the absence of pre-B cell receptor formation

Contents lists available at ScienceDirect

Biochemical and Biophysical Research Communications

Distorted antibody repertoire developed in the absence of pre-B cell receptor formation

Lin Sun [a, f], Naoko Kono [b], Takeyuki Shimizu [c], Hiroyuki Toh [d], Hanbing Xue [a, f], Osamu Numata [e], Manabu Ato [f], Shigeyuki Itamura [b], Kazuo Ohnishi [f, *]

[a] Graduate School of Life and Environmental Sciences, University of Tsukuba, Tsukuba, Ibaraki 305-8572, Japan
[b] Center for Influenza Virus Research, National Institute of Infectious Diseases, Musashimurayama, Tokyo 208-0011, Japan
[c] Department of Immunology, Kochi Medical School, Kochi University, Nankoku, Kochi 783-8505, Japan
[d] School of Science and Technology, Kwansei Gakuin University, Sanda, Hyogo 669-1337, Japan
[e] Faculty of Life and Environmental Sciences, University of Tsukuba, Tsukuba, Ibaraki 305-8572, Japan
[f] Department of Immunology, National Institute of Infectious Diseases, Shinjuku, Tokyo 162-8640, Japan

ARTICLE INFO

ABSTRACT

The pre-B cell receptor (pre-BCR), consisting of the μ heavy chain (μHC) and the surrogate light chain (SLC, Vpre-B and λ5), plays important roles during B cell development. The formation of the pre-BCR, which enables the nascent immunoglobulin HC to associate with the SLC, is considered a prerequisite for B cell development. However, a significant number of peripheral mature (leaky) B cells exist in SLC-deficient mice. These leaky B cells develop in the absence of pre-BCR and do not undergo the pre-BCR checkpoint. The antibody repertoires of leaky B cells thus reflect the absence of pre-BCR function. To investigate how the absence of the pre-BCR is circumvented by these leaky-B cells and examine the effect of the pre-BCR checkpoint on the antibody system, we analyzed the antibody repertoires of λ5-deficient ($\lambda5^{-/-}$) mice using next-generation sequencing. In $\lambda5^{-/-}$ mice, spleen B cells displayed different patterns of VDJ-usage, relative to those in wild-type (WT) mice. Moreover, leaky B cells were neither derived from unusual B2 cells, characterized by particular LC gene rearrangements in the absence of pre-BCR signaling, nor from B1 cells, originating from different B cell progenitors. Analysis of the CDR-H3 amino acid sequences of μ-chain repertoires revealed that certain bone marrow B cells with particular CDR-H3 profiles undergo clonal expansion in $\lambda5^{-/-}$ mice. Part of these CDR-H3s contain arginine(s) in the middle of the CDR-H3 loop in $\lambda5^{-/-}$ mice, whereas few arginine(s) exist in this middle loop in WT CDR-H3s in the absence of clonal expansion. This CDR-H3 feature in $\lambda5^{-/-}$ mice presumably reflects the role of the pre-BCR in autoantibody regulation, since arginine(s) are often found in the antigen-binding site of auto-antibodies. Here, we present a unique viewpoint on the role of pre-BCR, by assessing the whole antibody repertoire formed in SLC-deficient mice.

1. Introduction

The recognition of antigens by antibodies represents a fundamental process of biological defense in vertebrates. Antibody-producing B cells develop in the bone marrow under various regulatory cues and form the repertoire of antigen-specific B cell clones [1]. The size of the antibody repertoire has been calculated as 10^{15} [2], which is too large to capture using preexisting immunological methods. However, the recent advent of next-generation sequencing (NGS) has achieved a breakthrough in the study of antibody repertoires [3,4]. We recently reported a simple method for visualizing the holistic view of mouse antibody repertoire dynamics using NGS [5].

B cells develop in the bone marrow, giving rise to a repertoire of antigen-specific clones and undergo a major differentiation checkpoint, mediated by the pre-B cell receptor (pre-BCR) [1]. The pre-BCR, which is composed of the immunoglobulin μ heavy chain

(Ig-μHC) and the surrogate light chain (SLC), containing Vpre-B and λ5, allows for progression of differentiation only in B cell precursors that have successfully undergone recombination at the IgH gene locus [6,7]. At this stage of development, the newly produced IgH assembles with the invariant SLC to form the pre-BCR, where the association with the SLC serves as a quality check for IgH [8,9]. The formation of the pre-BCR assesses not only the productivity of the nascent IgH, but also its autoreactivity [1,10,11].

λ5-deficient mice, which are phenotypically similar to those lacking Vpre-B or the entire SLC [12,13], are characterized by severe impairments in B cell development. However, this accompanies the characteristic generation of a significant number of mature B cells (leaky B cells). These leaky B cells develop in the absence of pre-BCR, implying that the repertoire of leaky B cells reflects the function of pre-BCR checkpoint.

To explore the role of pre-BCR in antibody formation, we used NGS to compare the full antibody repertoires of wild-type (+/+, WT) and $\lambda 5^{-/-}$ mouse littermates. The expansion of bone marrow B cells in $\lambda 5^{-/-}$ mice displayed characteristic repertoire patterns, suggesting a specific role for CDR-H3 sequences in the formation of antibody repertoires. Our approach uniquely addresses pre-BCR function in this context.

2. Materials and methods

2.1. Mice and ethics statement

The $\lambda 5^{-/-}$ mouse strain [12] was backcrossed for more than 10 generations to the C57BL/6 background, and maintained in specific-pathogen-free conditions. All animal experiments were performed according to institutional guidelines and with the approval of the National Institute of Infectious Diseases Animal Care and Use Committee (Permit Number: 213045-2).

2.2. Antibodies and reagents

See Supplementary materials.

2.3. Flow cytometry

See Supplementary materials.

2.4. Deep sequencing of antibody transcripts using NGS

NGS sequencing was performed as described previously, except that MiSeq was used instead of the Roche 454 system [5]. For additional details, please see Supplementary methods.

2.5. Visualization of V(D)J repertoires

Raw reads were quality-checked and filtered for reads longer than 200 bp, as previously described [5]. Briefly, read sequences were classified into antibody classes by searching for the class-specific CH1 sequence. The V_H, J_H, D_H, V_L, and J_L genes were annotated by using the standalone IgBlast program. IgH repertoires were visualized on the array on a three-dimensional mesh in which the x-axis represents 110× IGHV genes, and the y-axis represents 12× IGHD genes and the z-axis represents 4× IGHJ genes. IgL was visualized on the array on a two-dimensional diagram in which the x-axis represents 110× IGLVκ and 4× IGLVλ genes, and the y-axis represents 4× IGLJκ and 4× IGLJλ genes (Fig. S1). The volume of each sphere for IGH genes represents the number of reads classified on the node; the red spheres represent unannotated V-, D- and J-genes. Similarly, the length of each bar for IGL genes represents the number of reads classified on the node. The unannotated V- and J-

genes are represented on the right borderline.

2.6. Immunizations and ELISA

WT and $\lambda 5^{-/-}$ littermates were immunized intraperitoneally with 50 μg of NP_{39}-CGG precipitated with 100 μL of Imject Alum adjuvant (Thermo Scientific). For secondary antibody response experiments, littermates were immunized intravenously with 2.5 μg of NP_{39}-CGG 57 weeks later. The antibody titers were determined as described previously [14].

2.7. Amino acid sequence analysis of the CDR-H3 region

Amino acid sequences for the CDR-H3 region (IMGT-definition) were obtained for the IgBLAST output [15]. For each CDR-H3 sequence, we calculated the following two amino acid descriptors: 1) Kidera factor: these descriptors involve applying a multivariate analysis to the 188 physical properties of the twenty amino acids [16]. The factors were calculated using the "Kidera" function in the R package, Peptides v1.1.1 (Daniel Osorio). 2) Amino acid Weight in the Loop (AaWtLpR), relative index: we defined the index assessing the relative positions of specific amino acids in the CDR-H3 loops. For example, the relative position index of aspartic acid (Asp) in the CDR-H3 loop was calculated as follows:

$$WtLpR_{Asp} = \sum_{Asp} \left(1 - \left| \frac{\left(i - \frac{L}{2}\right)}{\left(\frac{L}{2}\right)} \right| \right) \quad (1 \leq i \leq L)$$

Where L is the length of CDR-H3 (in amino acids), and i is the position of the specific amino acid, Asp in this case, in the CDR-H3 loop. We calculated the WtLpR index for each of the twenty amino acids. Principal component analyses (PCA) were performed using the "princomp" function in R.

2.8. Multivariate analysis

Cluster analyses of VDJ and VJ profiles of individual mice were performed as described previously, using the "hclust" function in R ("ward" method with "canberra" distance) [5]. Pearson's correlation coefficients for IGHV usage were calculated between individual mice, using the array of IGHV usage frequency in each mouse.

3. Results

3.1. B cells generated in $\lambda 5^{-/-}$ mice

In $\lambda 5^{-/-}$ mice, significant numbers of peripheral B cells were observed, even though B cell development in the bone marrow is severely impaired in the absence of pre-BCR (Fig. 1A). Intriguingly, these B cells circumvented the pre-BCR checkpoint; hence, their development is pre-BCR-independent. These leaky B cells comprise 2.7% of blood lymphocytes, in ~1/20 of 4-week-old WT mice (52.2%), and reach approximately 10%, in ~1/5 of WT mice, by 25–30 weeks of age (Fig. 1B).

Initially, we considered two possible pathways for the generation of leaky B cells: 1) During the differentiation of B2 cells, a few precursor B cells may display a particular IgL, rearranged in the absence of pre-BCR, and differentiate into immature B cells, without extensive clonal expansion [12] (Fig. 1C (arrow 1)); 2) leaky B cells are generated from B1 cells derived from the neonatal liver [17] [18] or the peritoneal cavity [19]. Pre-BCR has little influence on B1 cell differentiation owing to the self-renewing properties of these cells [12] (Fig. 1C (arrow 2)). To address these potential pathways, we used NGS to analyze the sequences of antibody
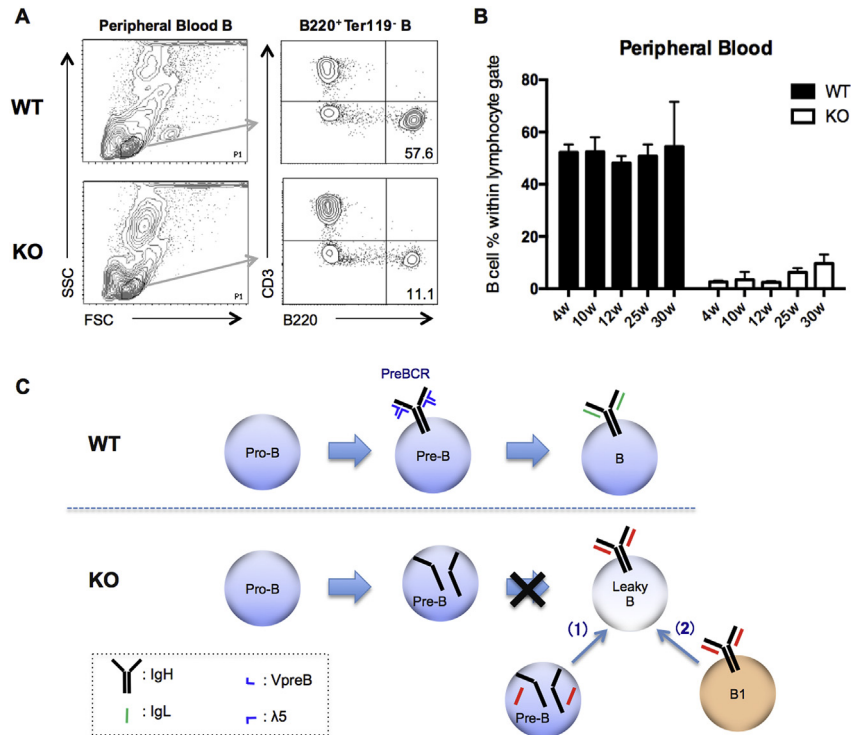
Fig. 1. Leaky B cells in the peripheral blood of KO ($\lambda5^{-/-}$) mice (A) Phenotypic analysis of peripheral blood B cells from WT and $\lambda5^{-/-}$ mice: peripheral B cells from littermates were collected from 4- to 30-week-old animals and analyzed by flow cytometry for B and T lymphocytes. Profiles in 30-week-old animals (B) Percentages of B220$^+$ B cells within the lymphocyte gate at the indicated ages (n = 38 (weeks 4—30)) (C) Two potential pathways for leaky B cell generation in $\lambda5^{-/-}$ mice, versus WT B cell development: according to pathway (1), a minority of pre-B cells undergo spontaneous LC gene rearrangements, in the absence of pre-BCR. According to pathway (2), leaky B cells originate from B1 cells derived from the fetal liver and/or peritoneal cavity.

transcripts for individual WT or $\lambda5^{-/-}$ littermates. More importantly, elucidation of the antibody repertoires in these leaky B cells should reveal the intrinsic role(s) of pre-BCR in the formation of the antibody system.

3.2. Different antibody repertoires form in WT and $\lambda5^{-/-}$ mouse littermates

Spleens from 9-week-old naïve WT and $\lambda5^{-/-}$ mice were used for analyzing the B cell repertoire of the IgM (Fig. 2A), IgG1 (Fig. S2) and IgG2c (Fig. S2) antibody subclasses. The VDJ-usage frequency profiles of naïve IgMs were highly correlated within each group of WT and $\lambda5^{-/-}$ mice. The VDJ repertoire of $\lambda5^{-/-}$ mice showed the preferential usage of certain IGH-V, such as the IGVH1-15 and 6-3 genes (Fig. 2A bottom panel), whereas WT mice commonly employed IGVH11-2, 4-1, and 7-3 (Fig. 2A bottom panel). Our cluster analysis of the class-switched IGH gene usage showed partial similarities, whereas the usage patterns for IgMs clearly differed between WT and $\lambda5^{-/-}$ littermates (Fig. 2B). Moreover, the VJ-usage profiles for Igκ and Igλ and the sequence similarities for the Igκ repertoires, examined by clustering, clearly differed between WT and $\lambda5^{-/-}$ littermates (Fig. S3).

3.3. IgH and IgL repertoire patterns in peripheral B cell subpopulations in WT and $\lambda5^{-/-}$ mice

To examine repertoire patterns in B cell subpopulations, especially B1 cells, spleen cells were sorted into follicular (FO) B cells, B1 cells, marginal zone (MZ) B cells, and transitional-2 (T2) B cells (Fig. 3A). The FO and the T2 cell counts were 3.4-fold and 11.2-fold higher, respectively, in the WT than those in $\lambda5^{-/-}$ mice, whereas

no differences were observed for the B1 and MZ cell counts (Fig. 3B). The IgH and IgL repertoires of these sorted B cell subpopulations were analyzed by NGS.

The FO, B1, MZ, and T2 B cell IgM VDJ repertoires (Fig. S4), and the similarities between WT and $\lambda5^{-/-}$ mice were assessed in each B cell compartment and analyzed by clustering (Fig. 3C). We detected two separate clusters, B1/T2 and MZ/FO, with similar WT and $\lambda5^{-/-}$ repertoires within each cluster, suggesting that $\lambda5^{-/-}$ FO cells are not derived from B1 cells. Similarly, the IgL (κ/λ) VJ repertoires were compared for the sorted cell populations (Fig. S5). The complexity of the $\lambda5^{-/-}$ IgL repertoires is comparable with that in WT mice, suggesting that leaky B cells in $\lambda5^{-/-}$ mice are not derived from precursor B cells in which the VJ-rearrangement occurred in the absence of pre-BCR. Cluster analysis also showed that the VJ repertoires of WT and $\lambda5^{-/-}$ mice were similar for each B cell compartment (Fig. 3D).

3.4. Different IgM repertoires are formed in the bone marrow of WT and $\lambda5^{-/-}$ mice

As our previous hypotheses regarding leaky B cell generation were refuted, we examined the bone marrow B cell repertoires for differences between WT and $\lambda5^{-/-}$ mice. The IgM repertoires of four WT and four $\lambda5^{-/-}$ littermates were analyzed (Fig. S6 and Fig. 4A). In WT mice, the VDJ combinations were relatively homogeneous, except that IGHV11-2 was preferentially used together with IGHJ1 and was commonly expanded in all four WT littermates. In $\lambda5^{-/-}$ mice, VDJ combinations were relatively sporadic and IGHV11-2 expansion was not observed in the littermates.

CDR-H3 sequences were deduced from IgBLAST outputs and compared between WT and $\lambda5^{-/-}$ mice. When CDR-H3 sequences
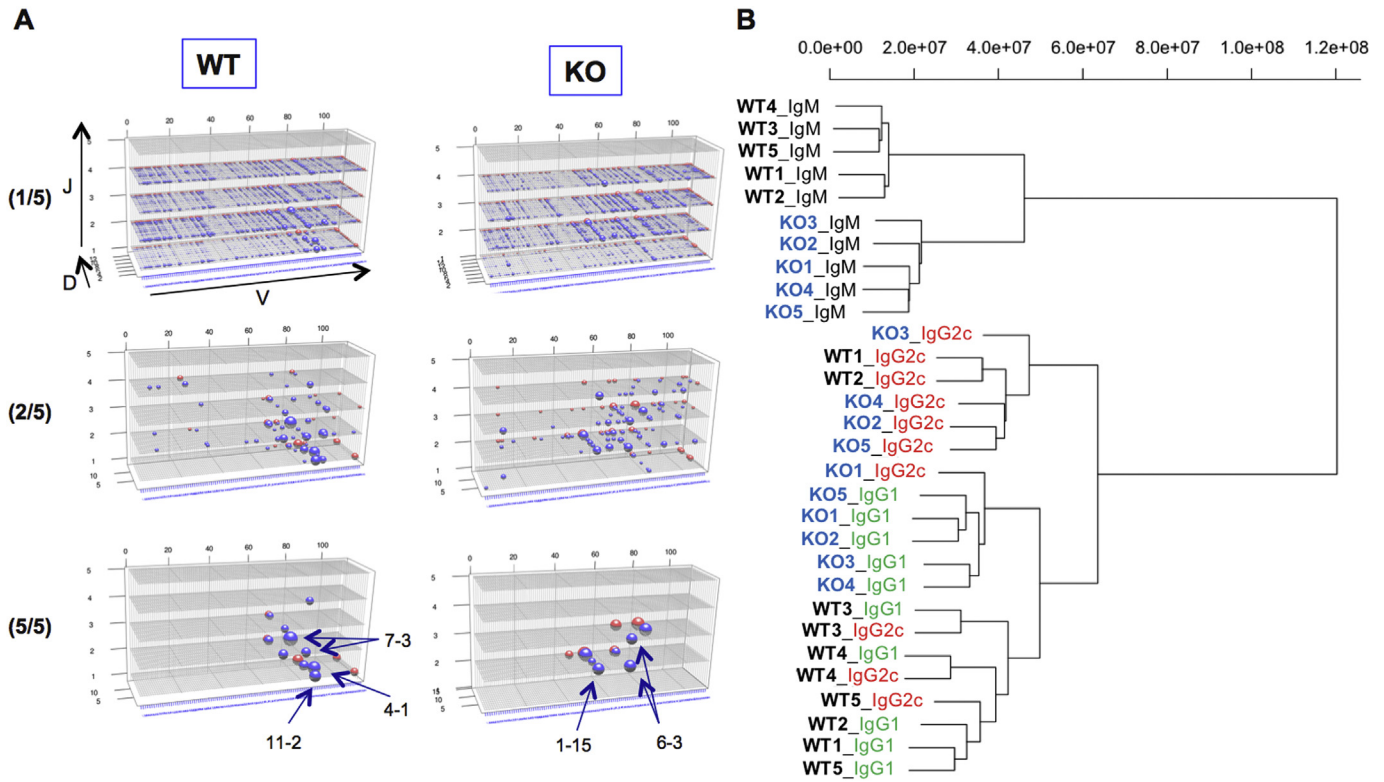
Fig. 2. NGS analysis of splenic B cell repertoires, showing specific profiles of different VDJ repertoires in WT and KO ($\lambda 5^{-/-}$) mice; VDJ distribution of IgM, IgG1, and IgG2c in the spleens of five WT and five $\lambda 5^{-/-}$ mice, analyzed by NGS (Fig. S2); visualization of 3D-VDJ-plots of holistic repertoires (see Materials and Methods). (A) IgM VDJ in 1/5 (top), 2/5 (center), and 5/5 mice (bottom). Major repertoires in WT (IGHV11-2, 4-1, and 7-3), and $\lambda 5^{-/-}$ mice (IGHV1-15, and 6-3), indicated by arrows (B) Cluster analysis of VDJ-usage in the IGH subclass of genes from five WT (WT1~5) and five $\lambda 5^{-/-}$ (KO1~5) spleens.
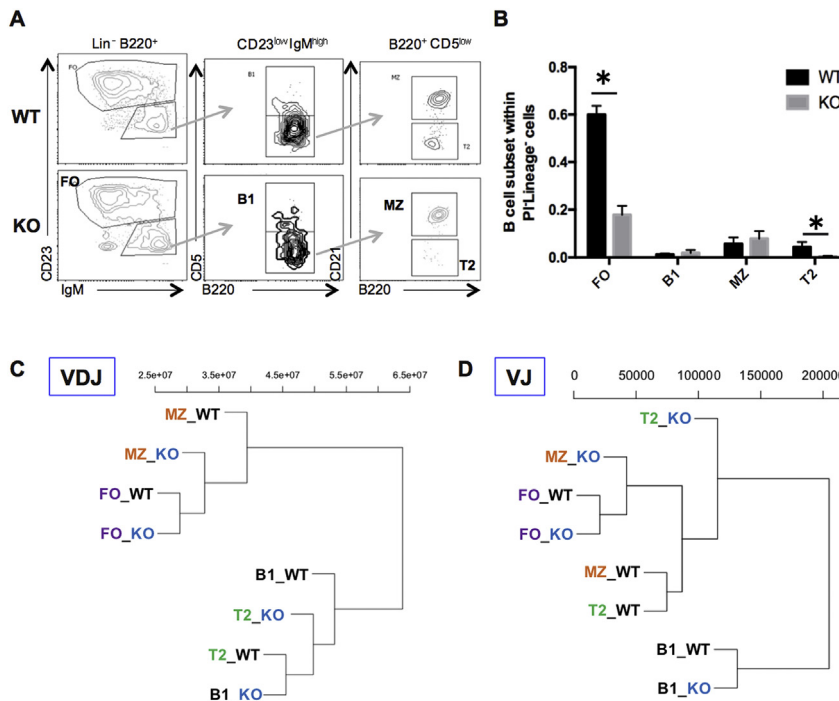
Fig. 3. IgH and IgL repertoire patterns of spleen B cell subpopulations in WT and KO ($\lambda 5^{-/-}$) mice (A) Spleen B cells from five pooled WT versus KO mice sorted into FO, T2, MZ, and B1 subpopulations (B) Comparison of frequencies of B cell subpopulations in WT and $\lambda 5^{-/-}$ mice. (*; $p < 0.05$, Student's t-test.) (C) Phylogenetic tree of IgM VDJ-usage distribution clusters in WT and $\lambda 5^{-/-}$ mice (D) Phylogenetic tree of IgL VJ-usage distribution clusters in WT and $\lambda 5^{-/-}$ mice.
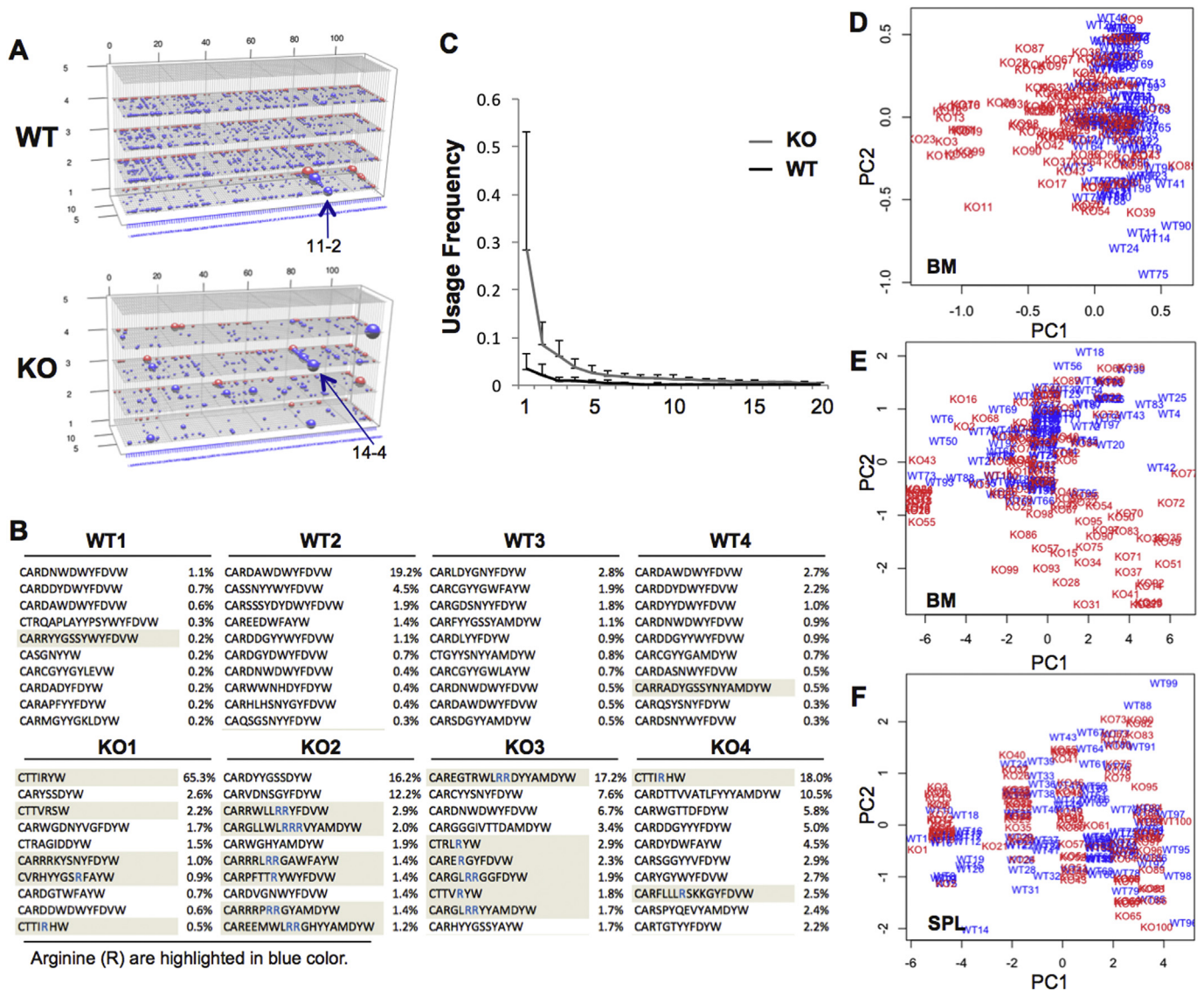
Fig. 4. Bone marrow-localized leaky B cells contain specific CDR-H3 repertoires. Bone marrow cells from five pooled WT and KO ($\lambda5^{-/-}$) mice were analyzed by NGS for VDJ-usage distribution. (A) VDJ-3D-plot of total bone marrow cells in WT and $\lambda5^{-/-}$ mice: representative pattern of four WT and $\lambda5^{-/-}$ littermates (see Fig. S6). The arrows indicate IGHV11-2 (in WT), and IGHV14-4 that was misread to IGHV11-2 (in $\lambda5^{-/-}$). (B) Amino acid sequences of CDR-H3 regions and frequencies in each mouse, listed in the order of their abundance; sequences containing Arg(s) in the middle are colored. (C) Frequency of CDR-H3 usage in WT and $\lambda5^{-/-}$ bone marrow cells: top 20 CDR-H3 sequences in each mouse, shown as in (B) (bars represent SD). (D) Amino acid descriptors (Kidera factors) calculated for the top 50 CDR-H3 amino acid sequences for each mouse and their discrepancy analyzed by Principal Component Analysis (PCA); values for WT (WT, blue) and $\lambda5^{-/-}$ (KO, red) mice, plotted on PC1 and PC2 axes. (E) Amino acid descriptors (AaWtLpR index) calculated for the same sequence as in (D) and analyzed by PCA as in (D). (F) Amino acid descriptors (AaWtLpR index) calculated for the top 50 CDR-H3 sequences in WT (blue) and $\lambda5^{-/-}$ spleens (KO, red), analyzed by PCA as in (D). (For interpretation of the references to colour in this figure legend, the reader is referred to the web version of this article.)

were sorted by abundance: the usage frequencies of top-ranking CDR-H3s were significantly higher in $\lambda5^{-/-}$ than in WT mice (Fig. 4B and C), suggesting the clonal expansion of restricted precursor B cell clones containing top-ranking CDR-H3 sequences.

To test whether the properties of the CDR-H3 amino acid sequences differed between WT and $\lambda5^{-/-}$ mice, we calculated physicochemical amino acid descriptors related to the 3D-protein structure [16,20], using Kidera factors, for each CDR-H3 sequence. Furthermore, we examined the differences between WT and $\lambda5^{-/-}$ mice using PCA. The physicochemical properties of CDR-H3s considerably differed between WT and $\lambda5^{-/-}$ mice (Fig. 4D), with the most dominant descriptor being "extended structure preference" in PC1 (Fig. S7). We next performed a PCA analysis of same CDR-H3 sequences (Fig. 4E), using factors expressing the relative position of each amino acid in the CDR-H3 loop (AaWtLpR, see

Materials and Methods). Interestingly, the major descriptor in PC2 was the relative position of arginines (Arg)s in the CDR-H3 loop (Fig. S8). Thus, the top-ranking CDR-H3 sequences in $\lambda5^{-/-}$ mice preferentially contain Arg(s) in the middle of the CDR-H3 loop, compared with those in WT (Fig. 4B, colored sequences). When bone marrow cells were sorted into pro/pre-B, immature B, and circulating B cell subsets (Fig. S9A), the Arg(s) in-the-middle-of-loop feature was not observed in pro/pre-B cells (Hardy's Fr. D, Fr. C and Fr. C') [21] but was evident in immature B (Fr. E) and recirculating B cells (Fr. F) (Fig. S9C). Thus, VDJ-recombination normally occurs in pro/pre-B cells in $\lambda5^{-/-}$ mice, while the μHC containing Arg(s) in the middle of the CDR-H3 loop was positively selected and retained in immature B cells. Interestingly, the dissociation of CDR-H3 profiles observed in bone marrow B cells was not observed between WT and $\lambda5^{-/-}$ spleen B cells (Fig. 4F), suggesting that the

distorted CDR-H3 repertoires were rectified during peripheral transition. Accordingly, investigation of the antibody response in WT and $\lambda 5^{-/-}$ mice by immunizing with the NP-CGG antigen revealed that the primary and secondary responses were not significantly different (Fig. S10A, B).

4. Discussion

To elucidate the role of pre-BCR in the formation of the antibody repertoire, we analyzed the full complement of BCR repertoires from spleens and bone marrows of WT and $\lambda 5^{-/-}$ mice using NGS. Our initial two hypothetical models for the pre-BCR-independent leaky B cell generation were refuted: leaky B cells are derived neither from the B1 cell compartment nor from the synthesis of a particular LC that compensates for SLC. In $\lambda 5^{-/-}$ bone marrows, substantial levels of productive IgM class VDJ-rearrangements were observed (Fig. 4A, Fig. S6).

Intriguingly, particular CDR-H3 sequences were preferentially enriched in IgM$^+$ B cells in $\lambda 5^{-/-}$ bone marrows (Fig. 4C). As it is unlikely for different clones to give rise to the same CDR-H3 sequence, the enrichment observed in $\lambda 5^{-/-}$ bone marrows suggests the clonal expansion of these precursor B cells in the absence of pre-BCR. When analyzing CDR-H3 properties using Kidera factors, differences in $\lambda 5^{-/-}$ CDR-H3s became obvious (Fig. 4D). This dissociation was also evident using simple amino acid descriptors calculated from the relative position of the twenty amino acids (Fig. 4E). Here, the most significant parameter was the relative position of Arg(s) in the CDR-H3 loop. In fact, about half of the top-ranking $\lambda 5^{-/-}$ CDR-H3 sequences contain Arg(s) in the middle of this loop, as opposed to that in WT sequences (Fig. 4B). When fractionating bone marrow B cells using Hardy's Fr. D (plus C and C′), Fr. E, and Fr. F, the dissociation of CDR-H3 sequences was not observed in Fr. D (plus C and C′), suggesting that the VDJ-rearrangement is not biased in the absence of $\lambda 5$. However, the dissociation becomes obvious in the Fr. E and Fr. F populations, suggesting that only a part of the non-biased VDJ-rearrangements in Fr. D, namely those containing the dissociated feature of CDR-H3s, passed the pre-BCR checkpoint (Fig. S9C).

These results suggest that the Arg(s) in the CDR-H3 loop compensate for the absence of SLC. We previously reported that an array of Args in the non-Ig portion of $\lambda 5$ induces receptor cross-linking and activates signaling in pre-B cells [22]. Thus, Arg(s) in the middle of the CDR-H3 loop may play a similar role and compensate for the absence of SLC, giving rise to leaky B cells. Unlike the other positively charged amino acids, Arg solubilizes protein aggregates [23]. It is therefore possible that the strong positive charge and potent solubilization ability of Arg underlie the specific interaction mode of biomolecules with the CDR-H3 loop.

However, about half of leaky B cells do not possess Arg(s) in the middle of the CDR-H3 loop (Fig. 4B), suggesting that other CDR-H3 features play similar roles in generating leaky B cells. We are currently investigating this second putative mechanism, including the properties of dissociated CDR-L3 sequences.

The pairing of the nascent IgH with the SLC configures an important checkpoint that controls and selects for IgH species [24–28]. CDR-H3 differences may affect the pairing ability of SLC. Therefore, Arg(s) in the CDR-H3 loop may impair SLC pairing and induce apoptosis in WT B cells, but not in $\lambda 5^{-/-}$ B cells. Thus, Arg-containing CDR-H3s would persist in the $\lambda 5^{-/-}$ repertoire. However, this explanation does not account for the clonal expansion of Arg-containing CDR-H3s (Fig. 4C).

Accumulating evidence suggests that the pre-BCR checkpoint prevents autoreactivity in nascent μHCs, acting as a surrogate autoreactive receptor [1,10,29]. In addition, the weak autoreactivity of pre-BCR may represent a driving force for the positive selection of B cells in the bone marrow [1,11]. Our data support this viewpoint. When assessing the whole repertoire of bone marrow μHC in $\lambda 5^{-/-}$ mice, only CDR-H3s with specific feature(s) passed the pre-BCR checkpoint, and autoreactive CDR-H3s (containing Arg(s)) were expanded in the absence of $\lambda 5$. These autoreactive μHC repertoires were negatively selected in the process of peripheral transfer (Fig. 4F) at the third and fourth checkpoint in B cell development [1]. However, these repertoires remained skewed, while peripheral VDJ repertoires were distorted in $\lambda 5^{-/-}$ mice (Fig. 2). Nevertheless, the antibody response against NP-CGG was comparable in WT and $\lambda 5^{-/-}$ mice, except for the ratio of the high-affinity IgM antibody (Fig. S10). These results suggest the presence of robust mechanism(s) for correction of skewed antibody repertoires. We are currently analyzing the mechanism underlying the selection of B cell clones with dissociated CDR-H3 sequences.

Transparency document

Transparency document related to this article can be found online at https://doi.org/10.1016/j.bbrc.2017.11.171.

Appendix A. Supplementary data

Supplementary data related to this article can be found at https://doi.org/10.1016/j.bbrc.2017.11.171.

References

[1] F. Melchers, Checkpoints that control B cell development, J. Clin. Invest. 125 (2015) 2203–2210.
[2] H.W. Schroeder Jr., Similarity and divergence in the development and expression of the mouse and human antibody repertoires, Dev. Comp. Immunol. 30 (2006) 119–135.
[3] G. Georgiou, G.C. Ippolito, J. Beausang, et al., The promise and challenge of high-throughput sequencing of the antibody repertoire, Nat. Biotechnol. 32 (2014) 158–168.
[4] J.A. Weinstein, N. Jiang, R.A. White, et al., High-throughput sequencing of the zebrafish antibody repertoire, Science 324 (2009) 807–810.
[5] N. Kono, L. Sun, H. Toh, et al., Deciphering antigen-responding antibody repertoires by using next-generation sequencing and confirming them through antibody-gene synthesis, Biochem. Biophys. Res. Commun. 487 (2017) 300–306.
[6] T. Tsubata, M. Reth, The products of pre-B cell-specific genes (lambda 5 and VpreB) and the immunoglobulin mu chain form a complex that is transported onto the cell surface, J. Exp. Med. 172 (1990) 973–976.
[7] H. Karasuyama, A. Kudo, F. Melchers, The proteins encoded by the VpreB and lambda 5 pre-B cell-specific genes can associate with each other and with mu heavy chain, J. Exp. Med. 172 (1990) 969–972.
[8] H. Karasuyama, A. Rolink, Y. Shinkai, et al., The expression of Vpre-B/lambda 5 surrogate light chain in early bone marrow precursor B cells of normal and B cell-deficient mutant mice, Cell 77 (1994) 133–143.
[9] F. Melchers, The pre-B-cell receptor: selector of fitting immunoglobulin heavy chains for the B-cell repertoire, Nat. Rev. Immunol. 5 (2005) 578–584.
[10] R.A. Keenan, A. De Riva, B. Corleis, et al., Censoring of autoreactive B cell development by the pre-B cell receptor, Science 321 (2008) 696–699.
[11] S. Herzog, H. Jumaa, Self-recognition and clonal selection: autoreactivity drives the generation of B cells, Curr. Opin. Immunol. 24 (2012) 166–172.
[12] D. Kitamura, A. Kudo, S. Schaal, et al., A critical role of lambda 5 protein in B cell development, Cell 69 (1992) 823–831.
[13] T. Shimizu, C. Mundt, S. Licence, et al., VpreB1/VpreB2/lambda 5 triple-deficient mice show impaired B cell development but functional allelic exclusion of the IgH locus, J. Immunol. 168 (2002) 6286–6293.
[14] S. Funakoshi, T. Shimizu, O. Numata, et al., BILL-cadherin/cadherin-17 contributes to the survival of memory B cells, PLoS One 10 (2015), e0117566.

[15] M.P. Lefranc, V. Giudicelli, C. Ginestoux, et al., IMGT, the international Im-MunoGeneTics information system, Nucleic Acids Res. 37 (2009) D1006–D1012.

[16] A. Kidera, Y. Konishi, M. Oka, et al., Statistical analysis of the physical properties of the 20 naturally occurring amino acids, J. Prot. Chem. 4 (1985) 23–55.

[17] T.A. Doran, R.J. Benzie, J.L. Harkins, et al., Amniotic fluid tests for fetal maturity, Am. J. Obstet. Gynecol. 119 (1974) 829–837.

[18] J.J. Owen, M.C. Raff, M.D. Cooper, Studies on the generation of B lymphocytes in the mouse embryo, Eur. J. Immunol. 5 (1976) 468–473.

[19] I.E. Godin, J.A. Garcia-Porrero, A. Coutinho, et al., Para-aortic splanchnopleura from early mouse embryos contains B1a cell progenitors, Nature 364 (1993) 67–70.

[20] M. Epstein, M. Barenco, N. Klein, et al., Revealing individual signatures of human T cell CDR3 sequence repertoires with Kidera Factors, PLoS One 9 (2014), e86986.

[21] R.R. Hardy, C.E. Carmack, S.A. Shinton, et al., Resolution and characterization of pro-B and pre-pro-B cell stages in normal mouse bone marrow, J. Exp. Med. 173 (1991) 1213–1225.

[22] K. Ohnishi, F. Melchers, The nonimmunoglobulin portion of lambda5 mediates cell-autonomous pre-B cell receptor signaling, Nat. Immunol. 4 (2003) 849–856.

[23] A. Hirano, T. Kameda, D. Shinozaki, et al., Molecular dynamics simulation of the arginine-assisted solubilization of caffeic acid: intervention in the inter-action, J. Phys. Chem. B 117 (2013) 7518–7527.

[24] E. ten Boekel, F. Melchers, A.G. Rolink, Changes in the V(H) gene repertoire of developing precursor B lymphocytes in mouse bone marrow mediated by the pre-B cell receptor, Immunity 7 (1997) 357–368.

[25] A.G. Rolink, T. Brocker, H. Bluethmann, et al., Mutations affecting either generation or survival of cells influence the pool size of mature B cells, Immunity 10 (1999) 619–628.

[26] R.R. Hardy, C.J. Wei, K. Hayakawa, Selection during development of V_H11^+ B cells: a model for natural autoantibody-producing $CD5^+$ B cells, Immunol. Rev. 197 (2004) 60–74.

[27] Y. Kawano, S. Yoshikawa, Y. Minegishi, et al., Selection of stereotyped V_H81X-μH chains via pre-B cell receptor early in ontogeny and their conservation in adults by marginal zone B cells, Int. Immunol. 17 (2005) 857–867.

[28] O. Grimsholm, W. Ren, A.I. Bernardi, et al., Absence of surrogate light chain results in spontaneous autoreactive germinal centres expanding V_H81X-expressing B cells, Nat. Commun. 6 (2015) 7077.

[29] N. Almqvist, I.L. Martensson, The pre-B cell receptor; selecting for or against autoreactivity, Scand. J. Immunol. 76 (2012) 256–262.